

Goldilocks RL: Tuning Task Difficulty to Escape Sparse Rewards for Reasoning

Ilia Mahrooghi^{†1}, Aryo Lotfi², and Emmanuel Abbe^{1,2}

¹*EPFL*

²*Apple*

Abstract

Reinforcement learning has emerged as a powerful paradigm for unlocking reasoning capabilities in large language models. However, relying on sparse rewards makes this process highly sample-inefficient, as models must navigate vast search spaces with minimal feedback. While classic curriculum learning aims to mitigate this by ordering data based on complexity, the right ordering for a specific model is often unclear. To address this, we propose Goldilocks, a novel teacher-driven data sampling strategy that aims to predict each question’s difficulty for the student model. The teacher model selects questions of appropriate difficulty for the student model, i.e., questions that are neither too easy nor too hard (Goldilocks principle), while training the student with GRPO. By leveraging the student’s performance on seen samples, the teacher continuously adapts to the student’s evolving abilities. On OpenMathReasoning dataset, Goldilocks data sampling improves the performance of models trained with standard GRPO under the same compute budget.

1 Introduction

The reasoning capabilities of Transformer-based models have been a focal point of recent research, with Reinforcement Learning (RL) emerging as a powerful paradigm for enhancing these abilities. Recent RL methods incentivize the generation of a detailed Chain of Thought (CoT) [29], enabling models to solve complex problems [36, 7, 28]. Additionally, increasing the computational budget at inference time, known as scaling test-time compute, has been shown to further enhance these reasoning capabilities [25, 17]. While RL has proven effective in unlocking complex reasoning behaviors, the computational efficiency of these methods remains a significant challenge. Recent findings by Khatri et al. [9] underscore that scaling is a fundamental driver of performance. This observation suggests that while models have the potential for continued improvement, realizing this potential through brute-force scaling is resource-intensive, making training efficiency a paramount concern.

Outcome Supervision (OS) [6, 34] further complicates this efficiency landscape. OS rewards the model only if the final answer is correct, creating a sparse reward signal where the model receives no feedback during the intermediate steps of reasoning. Because of this sparsity, the model is forced to explore a vast number of potential reasoning paths to stumble upon a correct solution. This need for extensive exploration to find a positive signal makes learning extremely slow and resource-intensive, serving as another critical motivation for improving the efficiency of RL training methods.

Curriculum Learning (CL) [4] offers a way to fix these inefficiencies by presenting training examples in a meaningful order instead of a random order. Recent studies, such as those by Qu et al. [20], Parashar et al. [19], Shen et al. [24], Chen et al. [5], and Yi et al. [33], have investigated various strategies to select and schedule data to improve the performance of language models. However, these CL methods cannot be used at the large scale of modern large language model training. Some existing approaches rely on tracking a model’s past performance on specific samples, which requires the model to check the same data points multiple times to estimate their difficulty. This “history-based” strategy struggles to generalize; it optimizes a schedule for datasets where the model sees examples many times, but it fails to judge the value of unseen data. Other works rely on the assumption that training data is

[†]Corresponding Author, ilia.mahrooghi@epfl.ch

categorized into distinct groups. This creates two problems: first, large-scale datasets usually lack clear categories; second, it incorrectly assumes that difficulty depends solely on the category, while it actually depends on the specific instance itself.

This limitation is particularly acute in the current landscape, where LLMs are trained on massive corpora that far exceed the scale of small, bounded benchmarks. In these large-scale settings, training efficiency is critical. Because the datasets are so huge, revisiting examples just to check their difficulty is a waste of valuable GPU resources. As a result, standard methods that rely on seeing data repeatedly are not practical. This creates a need for new strategies that can generalize, methods that can judge and schedule new data instantly without having to train on them first.

In this work, we propose **Goldilocks**, a teacher-driven framework, where in parallel to training a model (the student), a teacher continuously learns the student’s current capabilities and selects questions with appropriate difficulty for the student (questions that are neither too easy nor too hard). It generalizes to new data streams, which the student may not have seen, and builds a curriculum that matches best for the student at that time of training. With this framework, there is no need for the student to see each instance multiple times, and without relying on categorization assumptions, the teacher can generalize to new data streams.

The remainder of this paper is organized as follows: section 2 analyzes the gradient dynamics of Group Relative Policy Optimization (GRPO) [23] with verifiable rewards, establishing the theoretical link between outcome variance and the learning signal. section 3 introduces the architecture of the proposed Teacher and Student models. section 4 details the joint training framework, defining the data selection policy and the synchronized optimization loop. section 5 presents our empirical findings, demonstrating the efficiency gains and performance improvements of our approach. Finally, section 7 reviews related work, focusing on curriculum learning strategies within the context of reasoning tasks, and section 8 concludes the paper with a discussion on future research directions.

2 GRPO with Verifiable Reward

In the context of fine-tuning language models with RL, the objective is to maximize the expected reward on a dataset of verifiable answers. The standard policy gradient loss is defined as

$$L_{PG} = -\mathbb{E}_{s_t, a_t} \left[\log \pi_\theta(a_t | s_t) \hat{A}_t \right],$$

where π_θ denotes the policy and \hat{A}_t represents the estimated advantage. In the context of updating language models, the state s_t corresponds to the prompt q combined with the history of generated tokens $o_{<t}$, and the action a_t is the next token o_t . The objective is defined over the generated sequence of length T :

$$\mathcal{L}_{PG}(\theta) = -\mathbb{E}_{q \sim \mathcal{D}, o \sim \pi_\theta} \left[\sum_{t=1}^T \log \pi_\theta(o_t | q, o_{<t}) \hat{A}_t \right],$$

where \hat{A}_t represents the advantage estimated at token step t .

In GRPO [23], the advantage is computed by normalizing rewards across a group of outputs sampled for a single prompt. We decompose the total reward into two distinct components: a format compliance reward, r_{format} , and a binary verification reward, r_{ver} , where $r_{\text{ver}} = 1$ for a correct final answer and $r_{\text{ver}} = 0$ otherwise. The total reward is defined as

$$r_{\text{total}} = r_{\text{format}} + r_{\text{ver}}. \quad (1)$$

Assumption 1 (Format reward convergence). *There exists an iteration threshold $N \in \mathbb{N}$ such that for all training steps $t \geq N$, the component r_{format} becomes constant. This implies that the model eventually masters the required output structure, after which the format reward provides no further discriminative signal for learning.*

For a given question q , let p_q denote the probability that the model generates a correct solution (i.e., $r_{\text{ver}} = 1$). Consequently, the verification reward follows a Bernoulli distribution: $r_{\text{ver}} \sim \text{Bernoulli}(p_q)$.

The GRPO algorithm computes the advantage \hat{A}_q by standardizing the total reward, i.e.,

$$\hat{A}_q = \frac{r_{\text{total}} - \text{mean}(r_{\text{total}})}{\text{std}(r_{\text{total}})}.$$

Invoking Assumption 1, for sufficient training steps, the format reward stabilizes to a constant $r_{\text{format}} = C$. Since $r_{\text{ver}} \sim \text{Bernoulli}(p_q)$, the moments of the total reward become:

$$\text{mean}(r_{\text{total}}) = p_q + C \quad \text{and} \quad \text{std}(r_{\text{total}}) = \sqrt{p_q(1 - p_q)}.$$

Substituting these values, the advantage \hat{A}_q takes on two distinct values depending on the correctness of the output:

- **Correct answer** (probability p_q): The reward is $1 + C$, yielding:

$$\hat{A}_q = \frac{(1 + C) - (p_q + C)}{\sqrt{p_q(1 - p_q)}} = \frac{1 - p_q}{\sqrt{p_q(1 - p_q)}}.$$

- **Incorrect answer** (probability $1 - p_q$): The reward is C , yielding:

$$\hat{A}_q = \frac{C - (p_q + C)}{\sqrt{p_q(1 - p_q)}} = \frac{-p_q}{\sqrt{p_q(1 - p_q)}}.$$

Substituting these advantage values into the policy gradient objective, the loss L_{PG} for a specific question q can be expanded by explicitly separating the contributions of correct ($r_{\text{ver}} = 1$) and incorrect ($r_{\text{ver}} = 0$) outcomes:

$$\begin{aligned} \mathcal{L}_{PG} &= -\mathbb{E}_{q,o} \left[\sum_{t=1}^T \log \pi_\theta(o_t | q, o_{<t}) \hat{A}_t \right] \\ &= -p_q \mathbb{E} \left[\sum_{t=1}^T \log \pi_\theta(o_t | q, o_{<t}) \frac{1 - p_q}{\sqrt{p_q(1 - p_q)}} \middle| r_{\text{ver}} = 1 \right] - (1 - p_q) \mathbb{E} \left[\sum_{t=1}^T \log \pi_\theta(o_t | q, o_{<t}) \frac{-p_q}{\sqrt{p_q(1 - p_q)}} \middle| r_{\text{ver}} = 0 \right] \\ &= -\sqrt{p_q(1 - p_q)} \left(\mathbb{E} \left[\sum_{t=1}^T \log \pi_\theta(o_t | q, o_{<t}) \middle| r_{\text{ver}} = 1 \right] - \mathbb{E} \left[\sum_{t=1}^T \log \pi_\theta(o_t | q, o_{<t}) \middle| r_{\text{ver}} = 0 \right] \right). \end{aligned} \tag{2}$$

Computing the magnitude of the gradient with respect to the model parameters θ yields:

$$\|\nabla_\theta L_{PG}\| = \sqrt{p_q(1 - p_q)} \times \left\| \mathbb{E} \left[\sum_{t=1}^T \log \pi_\theta(o_t | q, o_{<t}) \middle| r_{\text{ver}} = 1 \right] - \mathbb{E} \left[\sum_{t=1}^T \log \pi_\theta(o_t | q, o_{<t}) \middle| r_{\text{ver}} = 0 \right] \right\|. \tag{3}$$

Observing Eq. 3, the gradient norm scales linearly with $\sqrt{p_q(1 - p_q)}$. This implies that the learning signal is maximized for questions with high outcome variance (i.e., where $p_q \approx 0.5$). This aligns with theoretical findings by Razin et al. [21], which demonstrate that the expected gradient vanishes when the reward standard deviation is small. Conversely, samples where the model is already certain (success rates nearing 0 or 1) yield smaller gradient magnitudes, contributing less effectively to the optimization process. A special case arises when $p_q = 0$ or $p_q = 1$ (i.e., the question is too hard or too easy); in these instances, $\sqrt{p_q(1 - p_q)} = 0$, causing the gradient to vanish entirely and resulting in no updates to the model. Motivated by this observation, the goal of our proposed Goldilocks Teacher is to avoid questions that are too easy or too hard and to find questions that lead to large learning signals, i.e., questions that are at the edge of solvability for the model and have a high $\sqrt{p_q(1 - p_q)}$.

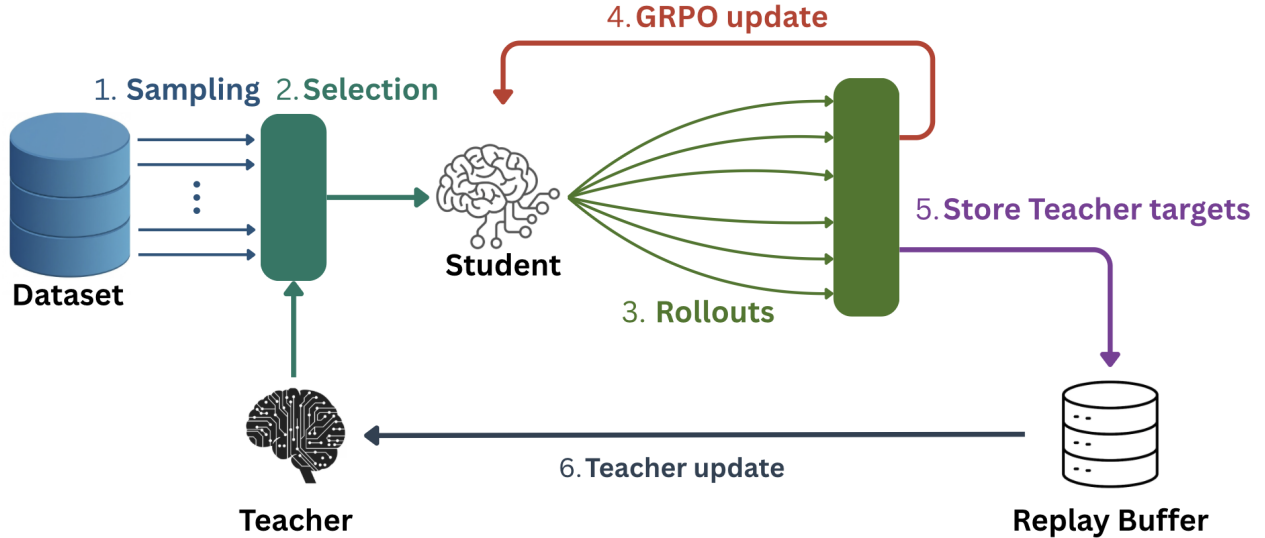


Figure 1: **Overview of the Goldilocks Framework.** The training cycle proceeds as follows: (1) A set of $K_{\text{candidate}}$ questions is sampled randomly from the dataset; (2) The Teacher selects the optimal prompt from this candidate pool; (3) The Student generates G rollouts for the selected prompt; (4) The gradient is calculated based on GRPO advantages and accumulated for the Student update; (5) Based on the empirical variance of the rollouts, Teacher targets are computed and stored in the replay buffer; (6) The Teacher is asynchronously updated using data sampled from the replay buffer.

3 Teacher and Student Architecture

3.1 Student

The Student model is initialized as a pretrained language model, parameterized by θ . It functions as the primary policy, denoted as $\pi_\theta(o | q)$, which maps an input question q to a generated output sequence o . This output typically consists of a reasoning chain followed by a final answer. The Student is fine-tuned via RL (specifically GRPO) to maximize the expected reward of its generated trajectories. Throughout the training process, the Student’s parameters are updated to improve the correctness of its reasoning, while serving as the source of feedback signals (success/failure) used to train the Teacher.

3.2 Teacher

The Teacher functions as a value predictor built upon a trainable language model backbone. For a given input question q , we extract the final layer embeddings and apply mean pooling to obtain a fixed-size vector representation. This vector is then passed through a linear projection layer. To strictly enforce the valid range of the standard deviation term (which lies between 0 and 0.5 for a Bernoulli variable), we apply a scaled sigmoid activation, i.e.,

$$f_\phi(q) = 0.5 \cdot \sigma(\mathbf{w}^T \cdot \text{MeanPool}(\text{Embed}(q)) + b),$$

where $f_\phi(q)$ represents the predicted utility of question q . The parameters ϕ encompass both the projection head and the pretrained language model, allowing the Teacher to learn deep semantic features relevant to difficulty estimation. For a detailed exploration of alternative teacher backbones and projection strategies, please refer to Appendix B.

4 Joint Training Procedure

We now detail the overall training loop, illustrated in Figure 1. The process operates in a cycle that alternates between data selection, student optimization via GRPO, and continuous teacher refinement.

4.1 Data Selection Policy (Steps 1-2)

During the data selection phase, the Teacher samples a candidate pool, denoted as \mathcal{C} , consisting of $K_{\text{candidate}}$ examples drawn randomly from the dataset. For each candidate question $q \in \mathcal{C}$, the Teacher computes a predicted utility score $\hat{v}_q = f_\phi(q)$. To balance exploration and exploitation, the final training sample q^* is selected using an ϵ -greedy strategy (Algorithm 1):

- With probability ϵ , a question is selected uniformly at random from \mathcal{C} to ensure diverse data coverage.
- With probability $1 - \epsilon$, the question with the highest predicted utility is selected deterministically, i.e.,

$$q^* = \arg \max_{q \in \mathcal{C}} \hat{v}_q.$$

Algorithm 1 Goldilocks Teacher: Data Selection Policy

```

1: Input: Dataset  $\mathcal{D}$ , Teacher Model  $f_\phi$ , Candidate Size  $K$ , Temperature  $\tau$ , Exploration  $\epsilon$ .
2: Output: Selected question  $q^*$ .
3: function SelectQuery( $\phi, \mathcal{D}$ )
4:    $\mathcal{C} \leftarrow$  Sample  $K$  random indices from  $\mathcal{D}$ 
5:    $\mathcal{V} \leftarrow \emptyset$ 
6:   for each candidate  $q \in \mathcal{C}$  do
7:      $\hat{v}_q \leftarrow f_\phi(q)$  {Predict learning utility}
8:      $\mathcal{V} \leftarrow \mathcal{V} \cup \{\hat{v}_q\}$ 
9:   end for
10:   $r \sim \text{Uniform}(0, 1)$ 
11:  if  $r < \epsilon$  then
12:     $q^* \leftarrow \text{Uniform}(\mathcal{C})$  {Ensure coverage ( $\epsilon$ -greedy)}
13:  else
14:     $q^* \leftarrow \arg \max_{q \in \mathcal{C}} \hat{v}_q$  {Greedy maximization}
15:  end if
16:  return  $q^*$ 
17: end function

```

4.2 Student Rollouts and Optimization (Steps 3-4)

Once the prompt q^* is selected, the Student model generates a group of G rollouts, $\{o_1, \dots, o_G\}$. The rewards are computed for each output as defined in Eq. 1, and the advantages are estimated using the group-relative normalization. Based on these advantages, the gradient is computed. To ensure optimization stability, gradients are accumulated over a batch of selected prompts before a parameter update is applied to the Student model.

4.3 Teacher Refinement (Steps 5-6)

The Teacher is trained online to predict the learning potential of specific prompts based on the Student's real-time feedback. Following the Student's rollouts for a question q , we calculate the empirical success rate \hat{p}_q as the fraction of correct solutions within the generated group. The regression target y_q is then set to the empirical standard deviation of the verification reward:

$$y_q = \sqrt{\hat{p}_q(1 - \hat{p}_q)}.$$

This tuple (q, y_q) is pushed into a replay buffer $\mathcal{D}_{\text{replay}}$ of capacity N_{replay} , which operates as a sliding window to retain the most recent interaction data.

The Teacher updates its parameters ϕ periodically as detailed in Algorithm 2. After every M_{update} samples processed by the Student, the Teacher undergoes a dedicated training phase lasting E_{teacher} epochs. During this phase, we iterate over the entire replay buffer $\mathcal{D}_{\text{replay}}$, processing the data in mini-batches \mathcal{B} to minimize the Mean Squared

Error:

$$\mathcal{L}_{\mathcal{B}}(\phi) = \frac{1}{|\mathcal{B}|} \sum_{(q, y_q) \in \mathcal{B}} (f_{\phi}(q) - y_q)^2.$$

This objective ensures the Teacher continuously aligns its predictions with the Student’s evolving capabilities.

5 Experiments and Results

To validate Goldilocks, we conduct a comprehensive evaluation using the OpenMathReasoning dataset [14], which comprises over 3 million chain-of-thought problems. Additional dataset details are in Appendix D. We train models using the GRPO algorithm across diverse model families, including Qwen2.5-1.5B [31], Qwen3-4B [32], Phi-4-mini-instruct (a 4B model) [2], and Olmo2-1B [16]. All experiments were implemented using the TRL library [27].

5.1 Experimental Setup

For all experimental configurations, we employ the selected open-weight models as Student policies, optimizing them via GRPO with a fixed group size of $G = 16$. We adopt a stratified strategy for Teacher instantiation: for compact architectures (Qwen2.5-1.5B and Olmo2-1B), the Teacher is initialized from the same base model as the Student. Conversely, for the larger 4B-parameter models (Phi-4-mini-instruct and Qwen3-4B), we utilize the Qwen3-1.7B [32] model as the Teacher to evaluate cross-model curriculum generation. Comprehensive implementation details are provided in Appendix A.

In all experiments, we utilized a fixed computational budget of 8 GPUs. For the GRPO baseline, all 8 GPUs were dedicated to the policy model. In contrast, the Goldilocks framework allocated 2 GPUs to the Teacher for dynamic data selection and 6 GPUs to the Student for training. Crucially, to isolate the efficacy of the curriculum strategy, we maintained identical global batch sizes and hyperparameters across both configurations. To ensure a fair comparison of computational cost, we normalize the training steps based on the effective resource allocation; specifically, we compare step n of the Goldilocks Student against step $\frac{8}{6}n$ of the baseline, strictly accounting for the difference in available compute for them.

Algorithm 2 Goldilocks Teacher: Online Refinement

```

1: Input: Question  $q$ , Rollouts  $\{r_1, \dots, r_G\}$ , Teacher Model  $f_{\phi}$ , Replay Buffer  $\mathcal{D}_{\text{replay}}$ , Capacity  $N_{\text{replay}}$ .
2: function UpdateTeacher( $q, \{r_i\}_{i=1}^G$ )
3:    $\hat{p}_q \leftarrow \frac{1}{G} \sum_{i=1}^G \mathbb{I}(r_i \text{ is correct})$  {Empirical success rate}
4:    $y_q \leftarrow \sqrt{\hat{p}_q(1 - \hat{p}_q)}$  {Compute target utility}
5:   Push  $(q, y_q)$  to  $\mathcal{D}_{\text{replay}}$ 
6:   if  $|\mathcal{D}_{\text{replay}}| > N_{\text{replay}}$  then
7:     Remove oldest sample from  $\mathcal{D}_{\text{replay}}$  {Sliding window}
8:   end if
9:   {Periodic Update Trigger (Step 6)}
10:  if Update Condition Met then
11:    Shuffle  $\mathcal{D}_{\text{replay}}$  and create batches  $\mathcal{B}$ 
12:    for epoch 1 to  $E_{\text{teacher}}$  do
13:      for batch  $B \in \mathcal{B}$  do
14:         $\mathcal{L} \leftarrow \frac{1}{|B|} \sum_{(q, y) \in B} (f_{\phi}(q) - y)^2$ 
15:         $\phi \leftarrow \phi - \eta \nabla_{\phi} \mathcal{L}$  {Gradient descent step}
16:      end for
17:    end for
18:  end if
19: end function

```

5.2 Main Results

Table 1 presents the performance benchmarks on the validation set of the OpenMathReasoning. Detailed specifications for the training step counts and the step-balancing logic between Goldilocks and the baselines are provided in Appendix A.5.

Table 1: **Performance on OpenMathReasoning.** We compare the Pass@1 accuracy of the Goldilocks against the GRPO baseline. Models denoted with \dagger employ a Qwen3-1.7B Teacher. The relatively low performance of the base model (without the RL training) is partly due to format issues.

Model	Base Model	Baseline (GRPO)	Goldilocks (Ours)
Olmo2-1B	2.5%	11.7%	14.9%
Qwen2.5-1.5B	13.48%	30.6%	33.4%
Qwen3-4B \dagger	12.4%	58.1%	59.7%
Phi-4-4B-Instruct \dagger	25.4%	37.1%	41.0%

For all reported validation accuracies, we average the last five validation steps to reduce statistical noise from both RL training and the evaluation itself, though accuracy plots are presented without denoising. All other training dynamics (e.g., student and teacher metrics) are smoothed using an Exponential Moving Average (EMA) with $\alpha = 0.9$.

Figure 2 depicts the validation accuracy curves throughout the optimization process, contrasting the baseline GRPO model Qwen2.5-1.5B with the Goldilocks Student Qwen2.5-1.5B and Teacher Qwen2.5-1.5B.

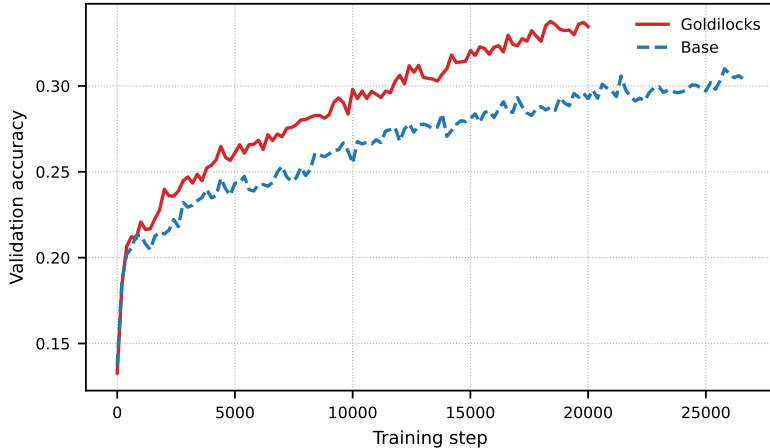


Figure 2: Evolution of validation accuracy over training steps.

5.3 Student Training Dynamics and Analysis

In this section, we examine the comparative training dynamics of the Goldilocks Student model relative to the GRPO baseline (for more figures see Appendix F). To understand the mechanism behind the improved performance, we first examine the evolution of the training success rate. Figure 3 compares the average of $r_{\text{validation}}$. Goldilocks exhibits a steeper slope, indicating accelerated learning. Moreover, the vertical offset confirms our sampling objective: the Teacher actively prioritizes questions where p_q is closer to 0.5, thereby maximizing the variance and learning signal.

As shown in Figure 4a, the Goldilocks maintains a consistently higher reward standard deviation. Consequently, as seen in Figure 4b, our method significantly reduces the fraction of questions with zero variance in their reward group (i.e., questions with $p_q(1 - p_q) = 0$, leading to zero gradients during GRPO). This ensures that the optimizer rarely wastes computation on samples that yield zero learning signal.

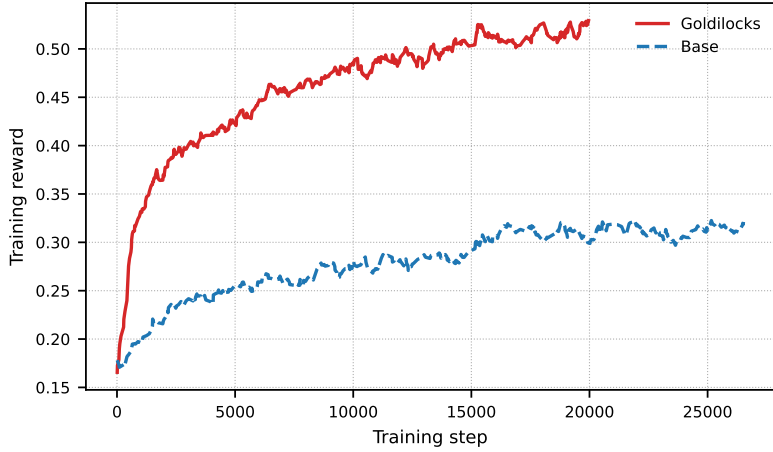


Figure 3: **Average Training Reward (Success Rate).** Goldilocks approach achieves higher training accuracy significantly earlier in training compared to the baseline.

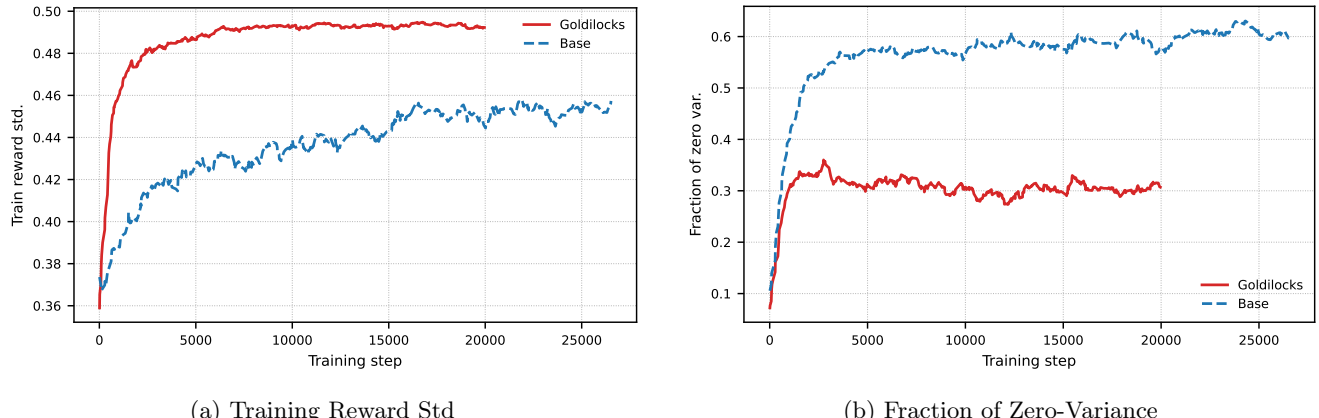


Figure 4: **Curriculum Mechanism.** (a) The Teacher actively selects samples with higher reward variance. (b) This results in far fewer “wasted” inputs where the gradient is zero.

The impact of active selection on the optimization landscape is quantified through the gradient norm dynamics. By prioritizing samples with higher uncertainty, Goldilocks maintains significantly larger gradient norms compared to the baseline (Figure 5). This stronger signal helps prevent optimization stagnation and ensures that the model performs more effective parameter updates per compute step, accelerating the learning process. This observation empirically validates the theoretical result derived in eq. (3), where we showed that the gradient norm maintains a linear relationship with the utility score $\sqrt{p_q(1 - p_q)}$.

5.4 Teacher Training Dynamics and Analysis

To validate the reliability of the Teacher’s scalar predictions, we conduct a fine-grained analysis of its optimization trajectory. The Teacher is trained to minimize the Mean Squared Error (MSE) between its predicted difficulty scores and the empirical ground truth derived from group rollouts.

Error Analysis on Unseen Samples. As detailed in section 4.3, the Teacher performs E_{teacher} epochs over batches sampled from the replay buffer. During each update cycle, we identify the subset of samples D_{new} that the Teacher has not yet encountered in previous training steps. We calculate the Mean Absolute Error (MAE) on this

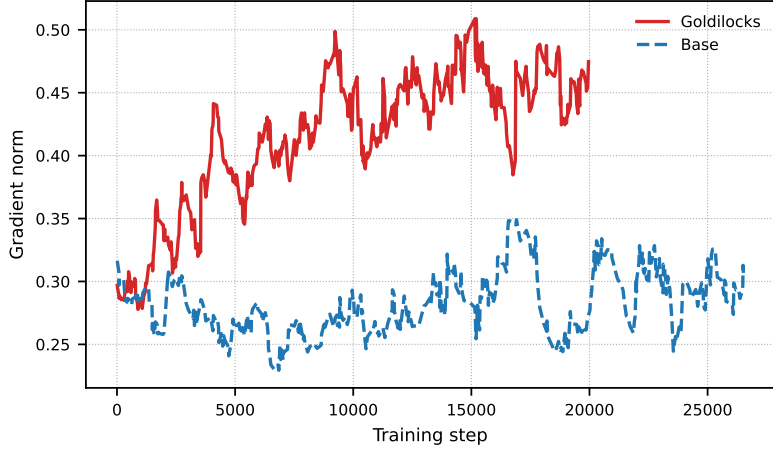


Figure 5: **Optimization Dynamics.** Goldilocks maintains larger gradient norms, preventing vanishing signals and providing a more robust optimization objective compared to the baseline.

specific subset during the first epoch of the update cycle as a proxy for validation loss, i.e.,

$$\mathcal{L}_{MAE}(\phi) = \frac{1}{|D_{\text{new}}|} \sum_{(q, y_q) \in D_{\text{new}}} |f_{\phi}(q) - y_q|,$$

where y_q is the ground truth difficulty derived from the rollouts. Because these samples are novel to the Teacher at the moment of evaluation, this metric effectively serves as an online validation score. We observe that this validation loss decreases consistently alongside the training MSE, indicating that the Teacher generalizes well rather than memorizing the replay buffer. Figure 6 compares the Teacher’s error across all samples against its error on samples that were not useful for the student (where $r_{\text{ver}} = 0$ or $r_{\text{ver}} = 1$ for all rollouts). The plot illustrates that the Teacher effectively learns to track and predict the evolving capabilities of the Student throughout the training process.

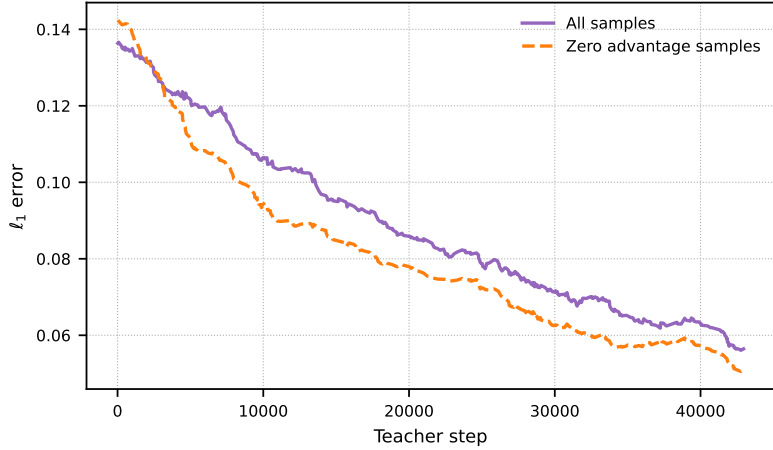


Figure 6: Teacher Mean Absolute Error (MAE) on unseen samples.

Prediction Distribution Monitoring. Beyond regression accuracy, we continuously track the distributional properties of the Teacher’s outputs. As the Teacher evaluates the stream of candidates to compute the Goldilocks score (\hat{y}_q), we log the mean (μ) and standard deviation (σ) of these predictions. Figure 7 illustrates the temporal evolution of these statistics, with the shaded region representing the standard deviation around the mean. A

sustained variance (σ) confirms that the Teacher continues to differentiate between sample difficulties throughout the training process, thereby avoiding mode collapse.

As training progresses, the student increasingly masters a larger portion of the dataset. Consequently, a growing number of samples yield consistently correct rollouts, rendering them less useful for further optimization and causing the ground-truth utility y_q to decrease. Figure 7 demonstrates that the mean (μ) of the Teacher’s predictions aligns with this trend, showing a downward trajectory over time. This alignment confirms that the Teacher is dynamically adapting to the student’s evolving capabilities throughout the training procedure rather than remaining static.

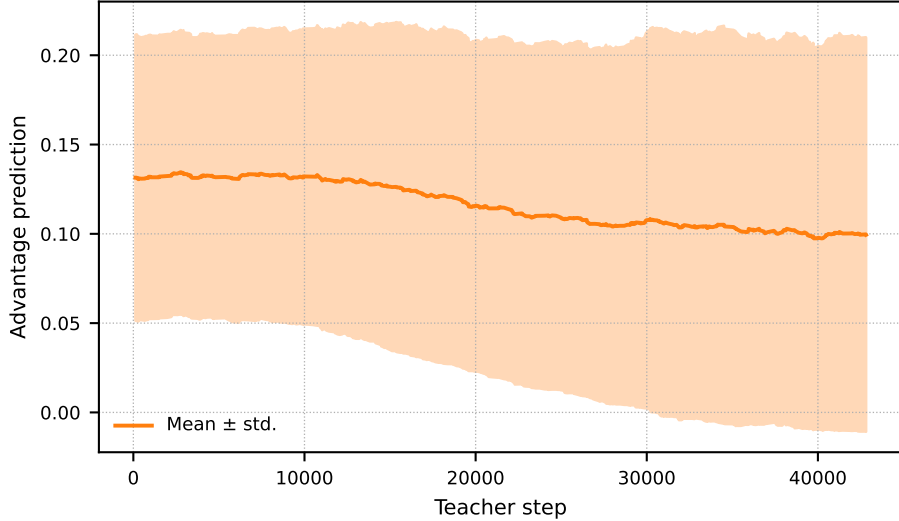


Figure 7: **Evolution of Teacher Predictions.** The mean (μ) of predicted Goldilocks score with the shaded region representing the standard deviation (σ).

6 Ablation Study

To assess the versatility of Goldilocks, we conduct two independent ablation experiments using the Qwen2.5-1.5B model. These experiments isolate the impact of our curriculum strategy when paired with advanced loss formulations and explicit regularization terms. The detailed training plots for these experiments are provided in Appendix C.

DAPO Loss. First, we evaluate the framework using the DAPO (Decouple Clip and Dynamic Sampling Policy Optimization) loss [35], which refines the standard group-based optimization by enforcing mixed-quality batches. Unlike GRPO, DAPO explicitly constrains the sampled group $\{o_i\}_{i=1}^G$ to contain at least one correct and one incorrect solution (i.e., $0 < \text{correct count} < G$). The loss is computed by normalizing the clipped surrogate objective over the total token count of the group:

$$\mathcal{L}_{\text{DAPO}}(\theta) = \mathbb{E} \left[\frac{1}{\sum_{i=1}^G |o_i|} \sum_{i=1}^G \sum_{t=1}^{|o_i|} \min \left(r_{i,t}(\theta) \hat{A}_{i,t}, \text{clip} \left(r_{i,t}(\theta), 1 - \epsilon_{\text{low}}, 1 + \epsilon_{\text{high}} \right) \hat{A}_{i,t} \right) \right]$$

where $r_{i,t}(\theta)$ is the probability ratio $\frac{\pi_\theta(o_{i,t}|\cdot)}{\pi_{\theta_{\text{old}}}(o_{i,t}|\cdot)}$ and the advantage $\hat{A}_{i,t}$ is derived via group-wise normalization $\frac{R_i - \text{mean}(\{R\})}{\text{std}(\{R\})}$. We train both the baseline and the Goldilocks student using this formulation while keeping all other hyperparameters constant. As shown in Table 2, Goldilocks retains its performance advantage, demonstrating that our curriculum-based data selection provides benefits orthogonal to the specific alignment loss employed.

Entropy Regularization. In a separate experiment, we investigate the effect of entropy regularization on the standard GRPO objective. In this context, the policy entropy $\mathcal{H}(\pi_\theta(\cdot|x))$ quantifies the diversity of the generated reasoning paths. We introduce an entropy bonus coefficient β to the loss function:

$$\mathcal{L}_{total} = \mathcal{L}_{GRPO} + \beta \mathbb{E}_{x \sim \mathcal{D}} [\mathcal{H}(\pi_\theta(\cdot|x))]. \quad (4)$$

Maximizing this term prevents premature convergence by encouraging the model to explore a wider range of solution paths. We compare the baseline against Goldilocks with a fixed coefficient of $\beta = 0.0003$. The results, presented in the bottom section of Table 2, indicate that even when both models are forced to explore via regularization, Goldilocks maintains its performance advantage.

Table 2: **Ablation Studies on Qwen2.5-1.5B.** We report the performance of Goldilocks and the GRPO baseline across DAPO loss function and entropy regularization.

Setting	Method	Parameter	Accuracy (%)
Standard Reference	Baseline	—	27.6%
	Goldilocks (Ours)	—	29.48%
DAPO Loss	Baseline	—	26.7%
	Goldilocks (Ours)	—	28.0%
Entropy Regularization	Baseline	$\beta = 0.0003$	27.4%
	Goldilocks (Ours)	$\beta = 0.0003$	29.1%

7 Related Works

Reasoning, Scratchpads, and Chain-of-Thought. It is widely established that success on challenging reasoning problems requires models to perform intermediate computations rather than deducting final answers directly. Early work by Nye et al. [15] demonstrated that supervised training with “scratchpads” significantly improves performance on tasks like polynomial evaluation and code execution. The study by Wei et al. [29] formalized this as Chain-of-Thought (CoT) prompting, showing that language models can generate reasoning traces via in-context demonstrations without explicit training, while Kojima et al. [10] extended this capability to the zero-shot setting. Theoretically, Abbe et al. [1] put forward the notion of globality degree of a task as a hardness measure, showing that scratchpads can make learning more efficient by breaking the globality of a task. Furthermore, to improve robustness, Gao et al. [8] proposed training on mathematical abstractions of reasoning traces rather than natural language.

RL for Reasoning. Several studies have highlighted the difficulty of applying RL to structured reasoning tasks due to the complexity of the output space [26, 12]. Standard policy gradient approaches such as PPO [22, 18] and, more recently, GRPO [23] have been adapted to optimize CoT generation using outcome-based verification rewards. A central challenge in this domain is the sparsity of rewards; models must navigate vast search spaces with binary feedback (correct/incorrect), making sample efficiency a significant bottleneck [36]. Consequently, methods that can prioritize high-signal training data are essential for scaling these techniques.

Curriculum Learning in Reasoning. Curriculum learning addresses data inefficiency by organizing training samples to optimize the learning trajectory. In the context of LLM reasoning, recent strategies have focused heavily on identifying the “frontier” of model capability. While early Teacher-Student frameworks, such as the one by Matiisen et al. [13], explored this by having a teacher assign subtasks of a specific problem to the student, modern approaches adapt this to large-scale generation. Several new methods attempt to stabilize training by maintaining a target success rate; for instance, Qu et al. [20] model question difficulty using a Beta distribution to select samples near a target accuracy γ^* , while Shen et al. [24] employ Thompson sampling for similar objectives. Other works focus on maximizing the gradient signal directly. The approach by Chen et al. [5] prioritizes samples exhibiting high absolute advantage ($|\hat{A}_q|$) using exponential moving averages, while Li et al. [11] allocate rollout budgets to avoid samples with trivial outcomes that yield zero gradients. Finally, strategies such as those in Amani et al. [3] and Xi et al. [30] adopt a scaffolding approach, facilitating learning by initially providing partial solutions and progressively shortening these hints over time.

8 Conclusion

In this work, we introduced Goldilocks, a teacher-driven framework for the dynamic construction of training curricula in reasoning models. Unlike traditional strategies that rely on history-dependent metrics or restrictive auxiliary metadata, our approach generalizes to novel data. The Goldilocks Teacher predicts the learning potential of unseen questions directly, enabling robust performance on data streams that neither the Student nor the Teacher has previously encountered. By filtering out uninformative samples before the Student expends computational resources, Goldilocks significantly accelerates training convergence.

9 Future Work

The paradigm of zero-shot utility estimation opens several high-impact research directions. First, the variance-aware selection policy could be adapted to other complex domains, such as code generation or automated theorem proving. Most critically, this methodology holds potential for large-scale pretraining; dynamically filtering trillion-token corpora based on predicted utility could drastically reduce training costs while improving final model quality. To further maximize throughput, we are currently experimenting with different resource allocation strategies, specifically isolating the Teacher on a single GPU while dedicating seven GPUs to the Student.

References

- [1] Abbe, E., Bengio, S., Lotfi, A., Sandon, C., and Saremi, O. How far can transformers reason? the globality barrier and inductive scratchpad. *Advances in Neural Information Processing Systems*, 37:27850–27895, 2024.
- [2] Abdin, M., Aneja, J., Behl, H., Bubeck, S., Eldan, R., Gunasekar, S., Harrison, M., Hewett, R. J., Javaheripi, M., Kauffmann, P., et al. Phi-4 technical report. *arXiv preprint arXiv:2412.08905*, 2024.
- [3] Amani, M. H., Lotfi, A., Baldwin, N. M., Bengio, S., Farajtabar, M., Abbe, E., and West, R. Rl for reasoning by adaptively revealing rationales. *arXiv preprint arXiv:2506.18110*, 2025.
- [4] Bengio, Y., Louradour, J., Collobert, R., and Weston, J. Curriculum learning. In *Proceedings of the 26th annual international conference on machine learning*, pp. 41–48, 2009.
- [5] Chen, X., Lu, J., Kim, M., Zhang, D., Tang, J., Piché, A., Gontier, N., Bengio, Y., and Kamaloo, E. Self-evolving curriculum for llm reasoning. *arXiv preprint arXiv:2505.14970*, 2025.
- [6] Cobbe, K., Kosaraju, V., Bavarian, M., Chen, M., Jun, H., Kaiser, L., Plappert, M., Tworek, J., Hilton, J., Nakano, R., Hesse, C., and Schulman, J. Training verifiers to solve math word problems. *arXiv preprint arXiv:2110.14168*, 2021.
- [7] DeepSeek-AI, Liu, D., et al. Deepseek-r1: Incentivizing reasoning capability in llms via reinforcement learning. *arXiv preprint arXiv:2501.12948*, 2025.
- [8] Gao, S., Bosselut, A., Bengio, S., and Abbe, E. Abstral: Augmenting llms’ reasoning by reinforcing abstract thinking. *arXiv preprint arXiv:2406.11228*, 2024.
- [9] Khatri, D., Madaan, L., Tiwari, R., Bansal, R., Duvvuri, S. S., Zaheer, M., Dhillon, I. S., Brandfonbrener, D., and Agarwal, R. The art of scaling reinforcement learning compute for llms. *arXiv preprint arXiv:2510.13786*, 2025.
- [10] Kojima, T., Gu, S. S., Reid, M., Matsuo, Y., and Iwasawa, Y. Large language models are zero-shot reasoners. In *Advances in Neural Information Processing Systems*, 2022.
- [11] Li, Z., Chen, C., Yang, T., Ding, T., Sun, R., Zhang, G., Huang, W., and Luo, Z.-Q. Knapsack rl: Unlocking exploration of llms via optimizing budget allocation. *arXiv preprint arXiv:2509.25849*, 2025.
- [12] Lightman, H., Kosaraju, V., Burda, Y., Edwards, H., Baker, B., Lee, T., et al. Let’s verify step by step. *arXiv preprint arXiv:2305.20050*, 2023.

[13] Matiisen, T., Oliver, A., Cohen, T., and Schulman, J. Teacher–student curriculum learning. *IEEE transactions on neural networks and learning systems*, 31(9):3732–3740, 2019.

[14] Moshkov, I., Hanley, D., Sorokin, I., Toshniwal, S., Henkel, C., Schifferer, B., Du, W., and Gitman, I. Aimo-2 winning solution: Building state-of-the-art mathematical reasoning models with openmathreasoning dataset. *arXiv preprint arXiv:2504.16891*, 2025.

[15] Nye, M., Andreassen, A. J., Gur-Ari, G., Michalewski, H., Austin, J., Bieber, D., Dohan, D., Lewkowycz, A., Bosma, M., Luan, D., et al. Show your work: Scratchpads for intermediate computation with language models. *ICLR 2022*, 2021.

[16] OLMo, T., Walsh, P., Soldaini, L., Groeneveld, D., Lo, K., Arora, S., Bhagia, A., Gu, Y., Huang, S., Jordan, M., et al. 2 olmo 2 furious. *arXiv preprint arXiv:2501.00656*, 2024.

[17] OpenAI. Learning to reason with llms. <https://openai.com/index/learning-to-reason-with-llms/>, 2024. Accessed: 2025-01-20.

[18] Ouyang, L., Wu, J., Jiang, X., Almeida, D., Wainwright, C., Mishkin, P., et al. Training language models to follow instructions with human feedback. In *Advances in Neural Information Processing Systems*, volume 35, pp. 27730–27744, 2022.

[19] Parashar, S., Gui, S., Li, X., Ling, H., Vemuri, S., Olson, B., Li, E., Zhang, Y., Caverlee, J., Kalathil, D., et al. Curriculum reinforcement learning from easy to hard tasks improves llm reasoning. *arXiv preprint arXiv:2506.06632*, 2025.

[20] Qu, Y., Wang, Q., Mao, Y., Hu, V. T., Ommer, B., and Ji, X. Can prompt difficulty be online predicted for accelerating rl finetuning of reasoning models? *arXiv preprint arXiv:2507.04632*, 2025.

[21] Razin, N., Zhou, H., Saremi, O., Thilak, V., Bradley, A., Nakkiran, P., Susskind, J., and Littwin, E. Vanishing gradients in reinforcement finetuning of language models. *arXiv preprint arXiv:2310.20703*, 2023.

[22] Schulman, J., Wolski, F., Dhariwal, P., Radford, A., and Klimov, O. Proximal policy optimization algorithms. *arXiv preprint arXiv:1707.06347*, 2017.

[23] Shao, Z., Wang, P., Zhu, Q., Xu, R., Song, A., Xiao, M., et al. Deepseekmath: Pushing the limits of mathematical reasoning in open language models. *arXiv preprint arXiv:2402.03300*, 2024. Introduces GRPO.

[24] Shen, Q., Chen, D., Huang, Y., Ling, Z., Li, Y., Ding, B., and Zhou, J. Bots: A unified framework for bayesian online task selection in llm reinforcement finetuning. *arXiv preprint arXiv:2510.26374*, 2025.

[25] Snell, C., Lee, J., Xu, K., and Kumar, A. Scaling llm test-time compute optimally can be more effective than scaling llm parameters. *arXiv preprint arXiv:2408.03314*, 2024.

[26] Uesato, J., Kushman, N., Kumar, R., Song, F., Siegel, N., Wang, L., et al. Solving math word problems with process- and outcome-based feedback. In *arXiv preprint arXiv:2211.14275*, 2022.

[27] von Werra, L., Belkada, Y., Tunstall, L., Beeching, E., Thrush, T., Lambert, N., Huang, S., Rasul, K., and Gallouédec, Q. TRL: Transformers Reinforcement Learning, 2020. URL <https://github.com/huggingface/trl>.

[28] Wang, Z. et al. T1: Advancing language model reasoning through reinforcement learning and inference scaling. *arXiv preprint arXiv:2503.xxxxx*, 2025.

[29] Wei, J., Wang, X., Schuurmans, D., Bosma, M., Chi, E., Le, Q., and Zhou, D. Chain-of-thought prompting elicits reasoning in large language models. In *Advances in Neural Information Processing Systems*, 2022.

[30] Xi, Z., Chen, W., Hong, B., Jin, S., Zheng, R., He, W., Ding, Y., Liu, S., Guo, X., Wang, J., et al. Training large language models for reasoning through reverse curriculum reinforcement learning. *arXiv preprint arXiv:2402.05808*, 2024.

- [31] Yang, A., Yang, B., Hui, B., Zheng, B., Yu, B., Zhou, C., Li, C., Li, C., Liu, D., Huang, F., Dong, G., Wei, H., Lin, H., Tang, J., Wang, J., Yang, J., Tu, J., Zhang, J., Yang, J., Yang, J., Zhou, J., Bai, J., He, J., Lin, J., Dang, K., Lu, K., Bao, K., Yang, K., Yu, L., Li, M., Xue, M., Zhang, P., Zhu, Q., Men, R., Xu, R., Li, T., Liu, T., Fan, W., Ge, W., Deng, X., Zhou, X., Ren, X., Zhang, X., Li, X., Fan, Y., Tan, Y., Wan, Y., Gao, Y., Xie, Y., Wang, Z., Wang, Z., Xiang, Z., Li, Z., Gao, Z., Xu, Z., and Ye, Z. Qwen2.5 technical report. *arXiv preprint arXiv:2412.15115*, 2024. URL <https://arxiv.org/abs/2412.15115>.
- [32] Yang, A., Li, A., Yang, B., Zhang, B., Hui, B., Zheng, B., Yu, B., Gao, C., Huang, C., Lv, C., et al. Qwen3 technical report. *arXiv preprint arXiv:2505.09388*, 2025.
- [33] Yi, H., Wang, K., Li, Q., Yu, M., Lin, L., Xi, G., Wu, H., Hu, X., Li, K., and Liu, Y. Safer-vlm: Toward safety-aware fine-grained reasoning in multimodal models. *arXiv preprint arXiv:2510.06871*, 2025.
- [34] Yu, F., Gao, A., and Wang, B. Ovm, outcome-supervised value models for planning in mathematical reasoning. *arXiv preprint arXiv:2311.09724*, 2023.
- [35] Yu, Q., Zhang, Z., Zhu, R., Yuan, Y., Zuo, X., Yue, Y., Dai, W., Fan, T., Liu, G., Liu, L., et al. Dapo: An open-source llm reinforcement learning system at scale. *arXiv preprint arXiv:2503.14476*, 2025.
- [36] Zelikman, E., Wu, Y., Mu, J., and Goodman, N. Star: Bootstrapping reasoning with reasoning. In *Advances in Neural Information Processing Systems*, volume 35, pp. 15476–15488, 2022.

Appendix

This appendix is organized as follows. Section A details the implementation specifics, including training configurations, hardware requirements, and the client-server code architecture. Section C presents detailed training dynamics and ablation studies. Section D outlines the dataset sampling and preprocessing procedures. Finally, Section E provides the exact prompts used for model evaluation, and Section F contains extended visualizations across all model families.

A Implementation Details

A.1 Training Configuration

We maintain a consistent global batch size of 288 across all experiments. The training infrastructure varies slightly between methods to accommodate the teacher model in the Goldilocks framework. Specifically, the GRPO baseline is distributed across 8 GPUs, whereas the Goldilocks student is distributed across 6 GPUs (reserving resources for the teacher).

Gradient accumulation steps are dynamically adjusted to preserve the fixed global batch size of 288 based on the model size and available devices:

- **Small Models:** We use a per-device batch size of 4.
 - *Goldilocks (6 GPUs)*: Gradient accumulation is set to $288/(4 \times 6) = 12$ steps.
 - *GRPO (8 GPUs)*: Gradient accumulation is set to $288/(4 \times 8) = 9$ steps.
- **4B Models:** We use a per-device batch size of 3.
 - *Goldilocks (6 GPUs)*: Gradient accumulation is set to $288/(3 \times 6) = 16$ steps.
 - *GRPO (8 GPUs)*: Gradient accumulation is set to $288/(3 \times 8) = 12$ steps.

A.2 Hyperparameters

Table 3a lists the hyperparameters used for the Student model (and the GRPO baseline), while Table 3b details the specific hyperparameters for the Goldilocks Teacher.

Table 3: Hyperparameters for the experiments. Left: Student Policy and GRPO Baseline. Right: Goldilocks Teacher Model.

(a) Student Policy & GRPO Baseline		(b) Goldilocks Teacher Model	
Hyperparameter	Value	Hyperparameter	Value
Learning Rate	1.0×10^{-5}	Learning Rate	1.0×10^{-6}
Max Prompt Tokens	1024	Per-Device Batch Size	8
Max Completion Tokens	2048	Training Epochs per Update (E_{teacher})	4
Number of Generations (G)	16	Candidate Set Size ($K_{\text{candidate}}$)	8
Temperature (Sampling)	0.7	Epsilon (ϵ)	0.2
Temperature (Evaluation)	0.0	Replay Buffer Capacity (N_{replay})	64
KL Coefficient	0.0	Update Frequency (M_{update})	4
Update Iterations	1	Loss Function	MSE
LoRA	False		
Evaluation Frequency	200 steps		

A.3 Code Details

We implemented the framework using a decoupled client-server architecture to efficiently manage the interaction between the Student and Teacher models. We found that the most robust approach is to isolate these components into two distinct processes:

- **Teacher Process (Server):** Acts as a central server that manages the curriculum and the replay buffer. It listens for requests from the student process.
- **Student Process (Client):** Runs the standard RL loop. When a new training sample is required, the student sends a request to the teacher.

The communication workflow operates as follows:

1. **Sample Request:** The student requests a new problem q from the teacher. The teacher selects a question based on its current utility estimates and sends it to the student.
2. **Feedback Loop:** After the student generates rollouts and computes the rewards for q , it sends these results back to the teacher.
3. **Asynchronous Updates:** The teacher aggregates this feedback into its replay buffer. Once the number of received samples reaches, the teacher triggers its own optimization step to refine the utility predictor f_ϕ .

This design allows for flexible scaling, as the heavy computation of the student (generating rollouts) is decoupled from the logic of the teacher’s selection and update mechanism.

A.4 Hardware and Computational Cost

Our experiments were conducted using NVIDIA H100 and B200 GPUs. Specifically, the larger 4B model variants were trained on B200 nodes. The average training run was approximately 1000 GPU hours for both GRPO and Goldilocks framework.

A.5 Training Steps and Accuracy Reporting

Each model variant was trained for a fixed number of steps to ensure a fair comparison across experimental conditions. The total training steps for each model are detailed below:

Table 4: Training step counts for Goldilocks and Baseline configurations. Baselines are allocated $\frac{4}{3} \times$ the steps of Goldilocks.

Model	Goldilocks Steps	Baseline Steps
Olmo2-1B	20,000	26,800
Qwen2.5-1.5B	20,000	26,800
Qwen3-4B	8,000	10,800
Phi-4-mini-Instruct (4B)	14,400	19,200

B Ablation Studies on Teacher Architectures

In addition to the teacher configuration introduced in the main text, we investigated alternative architectural choices for the utility predictor f_ϕ . Specifically, we explored different embedding extraction methods and Parameter-Efficient Fine-Tuning (PEFT) strategies.

B.1 Embedding Extraction Strategy

While our primary method utilizes mean pooling over the final layer embeddings to obtain a comprehensive question representation, we also evaluated using only the final token embedding. Given that the teacher base models are

autoregressively pretrained, the final token should theoretically encapsulate the semantic summary of the sequence. However, empirical results showed that this approach was less robust than mean pooling.

B.2 LoRA-based Training

To reduce the computational overhead of the teacher model, we experimented with Low-Rank Adaptation (LoRA) instead of full-parameter fine-tuning. We employed a high-rank configuration with the following parameters:

- **Rank (r):** 256
- **Alpha (α):** 512
- **Dropout:** 0.01

Despite the high rank, this configuration failed to match the performance of the full-parameter teacher. We observed that the teacher’s ability to accurately predict the standard deviation of rewards was significantly diminished, likely because the fine-grained semantic features required for difficulty estimation are better captured through full-model updates

C Ablation Studies Plots

In this section, we provide the detailed training dynamics corresponding to the ablation experiments discussed in the main text.

C.1 Validation Accuracy

Figure 8 illustrates the evolution of validation accuracy on the held-out OpenMathReasoning validation set over the course of training. Goldilocks demonstrates a steeper learning curve compared to the GRPO baseline in all settings.

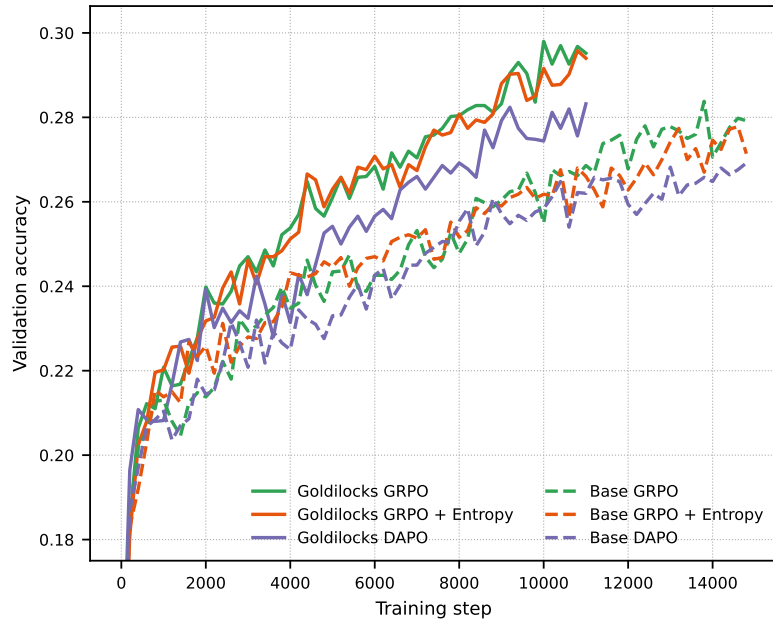


Figure 8: Validation accuracy over training steps.

C.2 Data Efficiency (Zero-Variance Fraction)

Figure 9 plots the fraction of training questions that yield zero variance in rewards (either all correct or all incorrect). Goldilocks consistently maintains a lower rate of zero-variance in all settings.

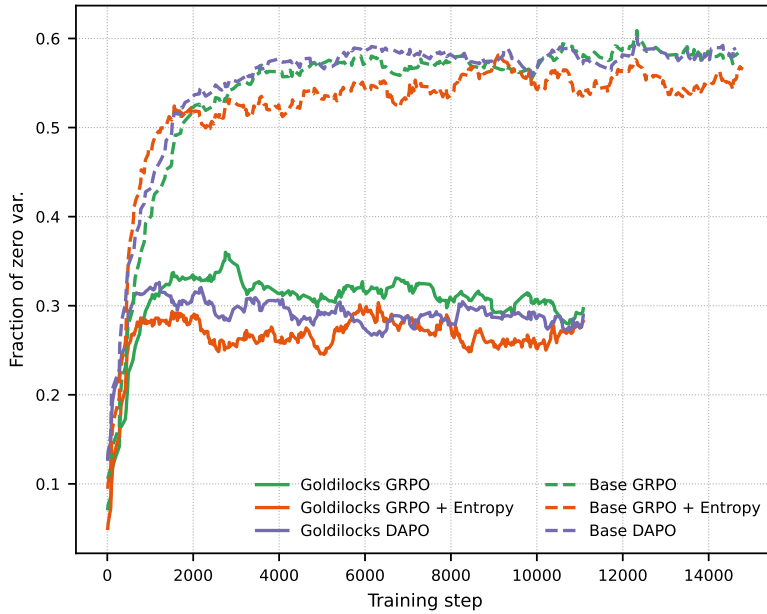


Figure 9: Fraction of questions yielding zero reward variance.

D Dataset Details

For our evaluation, we constructed a fixed validation set by randomly sampling 5,000 problems from the NVIDIA OpenMathReasoning dataset (<https://huggingface.co/datasets/nvidia/OpenMathReasoning>). To ensure a consistent comparison, this exact subset is used across all experiments.

Additionally, we applied a filtering step to ensure the reliability of automatic verification. Because some ground truth answers in the source dataset are difficult to parse purely by rules, we excluded any question where the parsed final answer resulted in a string length greater than 10. These cases typically correspond to formatting inconsistencies.

E Prompts

The final input to the model is constructed by concatenating a fixed header, the specific math problem, and a fixed footer:

$$\text{Input} = \text{PROMPT_HEADER} + \text{Question} + \text{PROMPT_FOOTER}$$

The exact text used for the header and footer is provided below.

Prompt Header

You are an expert problem solver. Your task is to solve the problem by explicitly showing your detailed Chain of Thought.

You must write out your reasoning step-by-step, explaining your logic

for every calculation or deduction.

Crucially, the final answer must be enclosed in a `\boxed{...}` command.

Prompt Footer

Strictly follow this output format:

Step-by-Step Reasoning

<Write your detailed thought process here. Do not skip steps.>

Final Answer

`\boxed{<your final answer>}`

Important: The `\boxed{...}` command should only contain the final, simplified numerical or symbolic answer, with no extra text or units.

F Extended Analysis of Training Dynamics

In this section, we provide additional visualizations of the training dynamics across evaluated model families. For each architecture, we present the evaluation accuracy on the validation set, the fraction of training samples yielding zero reward variance, and the mean training rewards.

F.1 Olmo2-1B Dynamics

Figure 10 illustrates the training progression for the Olmo2-1B model. Notably, the Goldilocks teacher successfully identifies samples that maintain the training reward near the optimal 0.5 threshold, minimizing redundancy and facilitating a more efficient climb in evaluation accuracy.

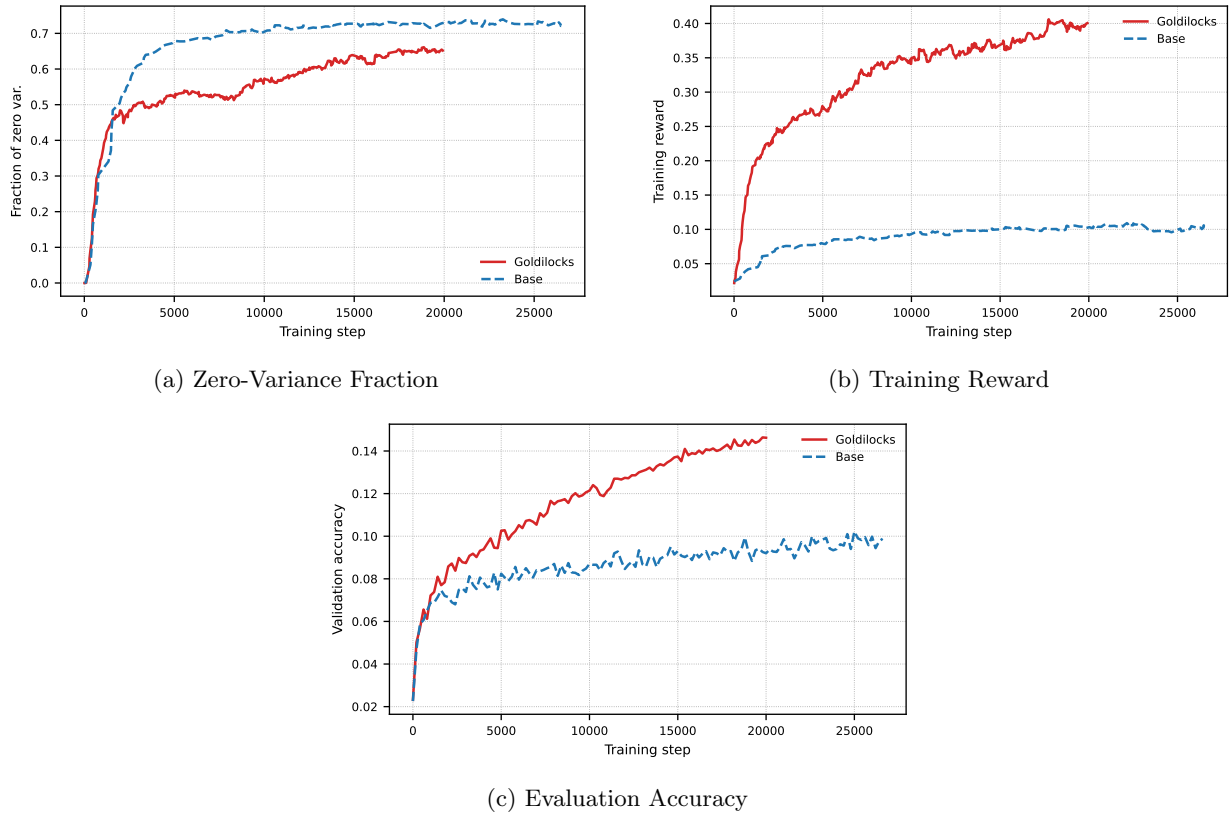


Figure 10: Training dynamics for Olmo2-1B.

F.2 Qwen3-4B Dynamics

The training dynamics for the Qwen3-4B model are presented in Figure 11. Specifically, the results demonstrate that even when the average reward exceeds 0.5, Goldilocks sampling actively shifts the distribution back toward the 0.5 threshold. This behavior effectively filters out “trivial” samples, those that the model has already mastered, thereby prioritizing questions with higher informational signal and reducing computational waste on solved instances.

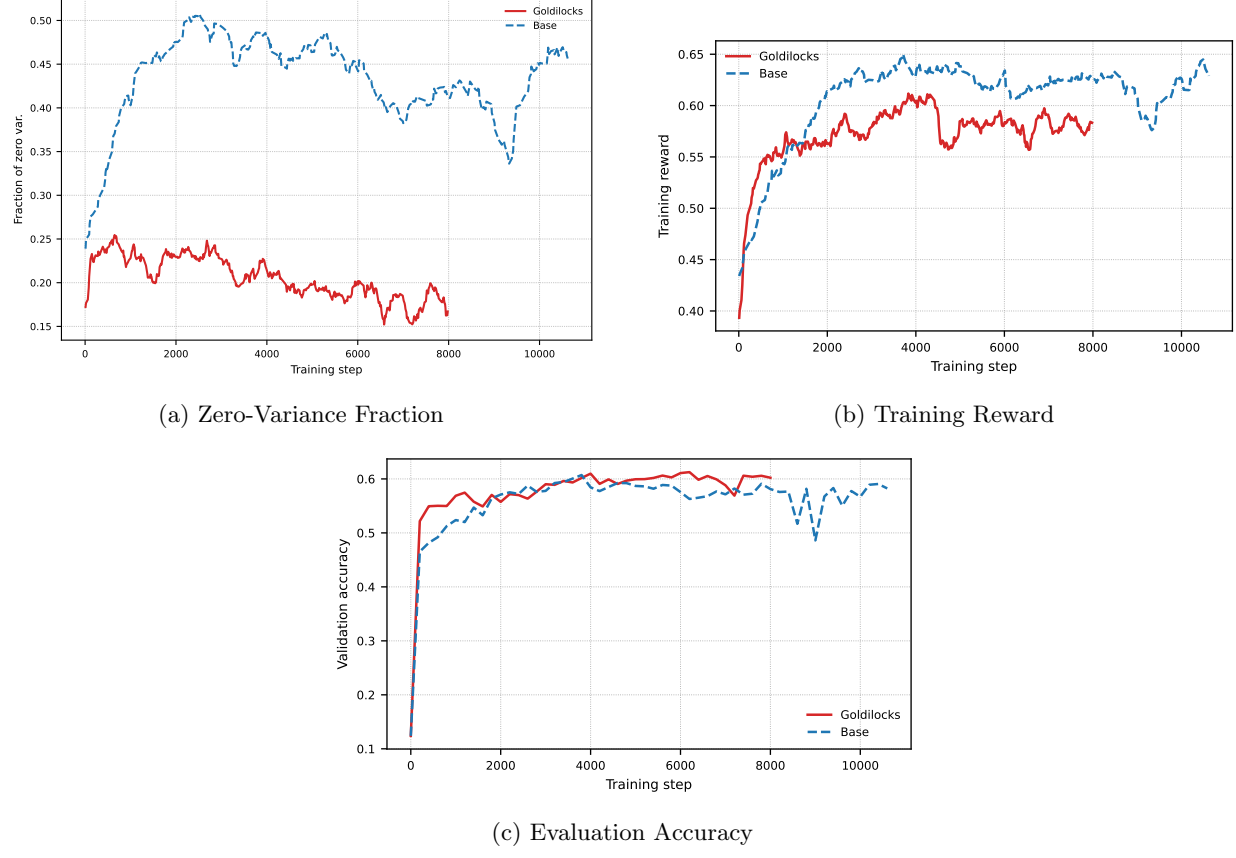


Figure 11: Training dynamics for Qwen3-4B.

F.3 Phi-4-mini-Instruct Dynamics

Figure 12 details the performance of the Phi-4-mini-Instruct model. The curriculum strategy significantly reduces the time spent on zero-variance samples, resulting in higher final validation set performance.

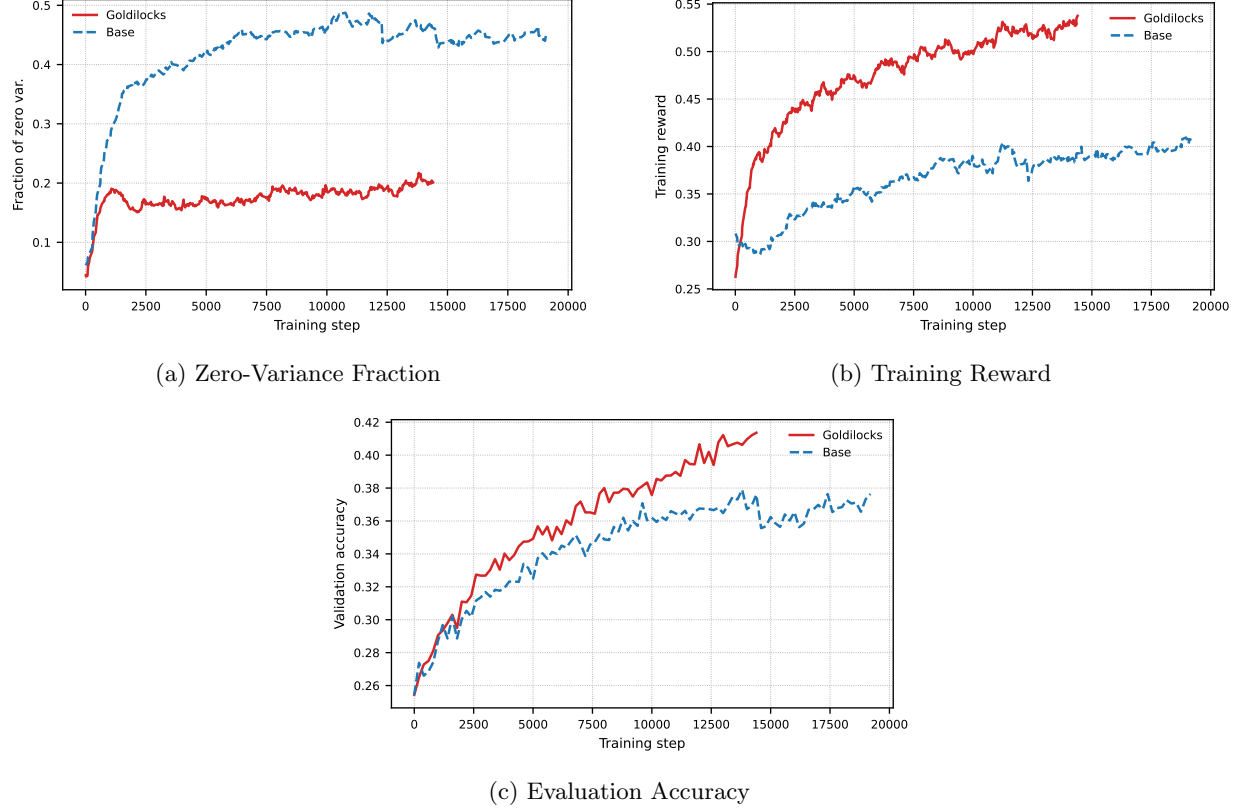


Figure 12: Training dynamics for Phi-4-mini-Instruct.